A Homogenization Technique to Calculate Eddy Current Losses in Soft Magnetic Composites Using a Complex Magnetic Permeability

Xiaotao Ren[1], Romain Corcolle[1,2], and Laurent Daniel[1]

[1]GeePs | Group of Electrical Engineering-Paris, CentraleSupélec, University of Paris-Sud. University of Paris-Saclay, Sorbonne University, Pierre-and-Marie-Curie University, Gif-sur-Yvette 91192, France
[2]New York University Shanghai, Shanghai 200122, China

Soft magnetic composites (SMCs) are a promising alternative to laminated steel in many electrical engineering applications. This is largely owing to their low level of eddy current (EC) losses. The electromagnetic behavior of SMC in electromagnetic devices cannot be easily predicted using standard numerical techniques, such as the finite-element (FE) method, mostly due to the computational cost required to model the material microstructure. Another difficulty lies in the high contrast between matrix and inclusion properties. In this paper, we propose a homogenization strategy to estimate EC losses in SMC. It is based on the calculation of a homogenized complex magnetic permeability. The imaginary part reflects the EC losses, while the real part describes the standard magnetic permeability. The complex permeability approach is applied to SMC with fiber or spherical inclusions. EC losses obtained from the complex permeability approach are compared with FE calculations, with very satisfying agreement.

Index Terms— **Cubic lattice, effective properties, heterogeneous materials, magnetic behavior, Maxwell Garnett (MG).**

I. Introduction

THE microstructure of soft magnetic composites (SMCs), consisting of ferromagnetic inclusions embedded in a dielectric polymer matrix, is at the origin of the low level of eddy current (EC) losses observed in these materials when they are subjected to electromagnetic loadings. This is why they are considered as a promising alternative to laminated steel, for instance, in motors [1]–[4].

In order to design electrical machines using SMC as magnetic material, the optimization of material properties is crucial. There are two dominant points to consider. First, a high magnetic permeability is required. Pure iron or Fe-alloys are then good candidates for the particle material [5]. Second, low EC losses are needed, and can be achieved because of the dielectric coating, which significantly cuts down the induced EC. Epoxy is often chosen as the matrix material. These constituents exhibit a very high contrast both in electric conductivity and magnetic permeability. This high property contrast is a serious challenge for homogenization techniques developed in order to deduce the effective properties of heterogeneous materials. However, these homogenization techniques are required to design optimal electromagnetic devices based on SMC.

SMC can be viewed microscopically as a periodic layout of inclusions embedded in a dielectric host matrix. The problem of determining the effective properties of periodic composites was first considered by Rayleigh [6]. He proposed a formula for the effective conductivity, based on a series expansion with coefficients determined from the rectangular lattice structure of the periodic pattern. But this model requires huge computation capacity to deal with the infinite sums involved. With the emergence of high-performance computing systems, Rayleigh's model [6] was discussed and extended [7], [8]. New approaches have also been proposed using complex analysis, based on the biperiodicity of elliptic functions on regular arrays of inclusions [9], [10]. These latter methods avoid the issue of summation of conditionally convergent series arising in Rayleigh's formula and provide an exact expression for the effective property tensor of composites with parallelogram lattice pattern. Nevertheless, these models are limited to 2-D configurations, since elliptic functions cannot deal with 3-D periodic problems.

Powerful computing capacity also enabled the rapid development of numerical strategies. One of the most commonly employed is the finite-element method (FEM). FEM provides a full-field approach to solve electromagnetic problems. Detailed information about the field distribution can be retrieved all over the study domain. Effective permeability, as well as losses, can then be post-processed. But in the case of SMC, the microstructure has to be finely meshed, and the brute FEM approach can bring significant numerical burden and instabilities. FEM homogenization techniques [11]–[13] have been introduced to tackle electromagnetic problems with different scales. The main idea is to replace periodic microstructures of composite by an equivalent homogeneous material. The equivalent homogeneous material can then be used in standard structural analysis tools, with a reduced numerical complexity. The properties of the equivalent homogeneous medium can be obtained through numerical computation. Various strategies derived from standard FEM have been proposed [14], [15]. These methods reduce the computational time and resources to a certain extent while maintaining accuracy.

Manuscript received May 12, 2016; revised July 13, 2016; accepted July 20, 2016. Date of publication July 26, 2016; date of current version November 16, 2016. Corresponding author: X. Ren (e-mail: xiaotao.ren@geeps.centralesupelec.fr).

Color versions of one or more of the figures in this paper are available online at http://ieeexplore.ieee.org.

Digital Object Identifier 10.1109/TMAG.2016.2594048

Nevertheless, these numerical methods still have the drawback of not being very flexible, for instance, for parametric studies that require multiple numerical computations. In addition, very high property contrast is difficult to address unless specific numerical techniques are used [15], [19]. Thus, it is crucial to develop new models for EC losses in SMC.

Semi-analytical homogenization [16] can be particularly suitable for SMC. The obtained equivalent homogeneous properties can be used in standard structural analysis tools. In the case of periodic microstructures, the asymptotic expansion technique [17], [18] can be used. But it requires heavy calculations of high-order correctors so as to attain high precision for local fields. Homogenization with second-order correctors can lead to inaccurate results [15].

An alternative branch of homogenization is mean field approaches. These analytical or semi-analytical techniques have, for instance, been developed for the determination of the effective magnetic permeability of ferromagnetic polycrystals [20], [21]. Analytical homogenization strategies have also been used for the determination of the effective permittivity of composites for shielding applications [22]–[24]. Préault *et al.* [24] developed a dynamic homogenization model (DHM) to extend the usage of homogenization models to a wide frequency range by introducing the ratio between the typical size of the microstructure and the typical length of the electromagnetic wave. DHM provides accurate results for shielding applications. Nevertheless, DHM, being an extension of Maxwell Garnett (MG) model [25], is confined in scope of usage to composite materials with low property contrast. Besides, although this model contains frequency information, it is inapplicable to determine EC. Indeed, these analytical or semi-analytical models pour attention only on the effective constitutive properties and do not provide an insight into losses characteristics of composites.

This paper presents a homogenization technique to estimate EC losses in composite materials with high contrast in constituent properties. It is based on the use of a complex magnetic permeability. Complex properties can be used in electromagnetic applications to describe dissipation. A thorough review of homogenization models for dielectric behavior using complex permittivity can be found in [26] and [27]. The 2-D and 3-D cases have been numerically explored in detail. The complex effective permittivity depends on the properties of each constituent, on their volume fraction and on their spatial arrangement [28]. In an analogous way, complex permeability is a useful tool to handle high-frequency magnetic effects, particularly for transformer applications [29], [30]. Power dissipation is directly reflected in the imaginary part of the complex permeability [31], [32]. In the case of SMC at low frequency, when the induced magnetic field can be neglected, there is no time lag between magnetic flux density and magnetic field. In this respect, the imaginary part of complex permeability should be considered as zero. However, EC losses are present—as long as the frequency is not zero. Thus, an imaginary part can be introduced into the magnetic permeability tensor so as to reflect EC losses. This paper focuses on the estimate of EC losses for SMC with linear behavior. Other types of losses, such as hysteresis losses and excess losses, are not considered.

In the first part, the definition of EC losses is briefly recalled, and the specificities of complex permeability tensor application are explained. In the second part, a strategy to handle these specificities is detailed, defining an effective complex permeability tensor for SMC. Finally, the results on EC losses are presented and compared with the FEM results.

II. Complex Magnetic Permeability for EC Losses

A. Definition of EC Loss Density

Consider a magnetic core (domain $\mathbf{\Omega}$) subjected to a magnetic field of frequency f. An induced electric field $\mathbf{E}$ appears in the conductive material with conductivity tensor $\bar{\bar{\sigma}}$, which further gives rise to EC losses in the material. The EC loss density $\mathcal{U}$ is defined as the Joule losses dissipated per unit volume during a wave period

$$\mathcal{U} = \frac{\langle \mathbf{E}^* \bar{\bar{\sigma}} \mathbf{E} \rangle}{2f} \tag{1}$$

where the superscript "$*$" refers to the conjugate transpose operator. The operator $\langle \cdot \rangle$ denotes a volume average over the domain $\mathbf{\Omega}$ by $\langle \cdot \rangle = (1/V) \int_V \cdot \, dV$, where V is the volume of $\mathbf{\Omega}$.

B. Complex Permeability Tensor

The complex permeability tensor $\tilde{\mu}$ ($\tilde{\mu} = \bar{\bar{\mu}}^r - j\bar{\bar{\mu}}^i$) can be used as a mathematical tool to represent a dissipative magnetic material. In this paper, we propose to use this complex permeability tensor to describe the effective properties of SMC. The real part is the usual magnetic permeability tensor, and the imaginary part reflects the EC losses.

Consider a homogeneous and linear material of permeability tensor $\tilde{\mu}$ excited by a harmonic magnetic field $\mathbf{H}(t) = \mathbf{H}_0 e^{j\omega t}$ ($\mathbf{H}_0$ is the magnetic field magnitude and ω is the angle frequency). The induction flux is $\mathbf{B}(t) = \tilde{\mu}\mathbf{H}_0 e^{j\omega t}$. As in the case of transformers at high-frequency range [32], the energy loss density in a period of time T is

$$\mathcal{S} = \frac{1}{2}\Re\left(\int_0^T \mathbf{H}^*(t)\frac{d\mathbf{B}(t)}{dt}\,dt\right) \tag{2}$$

where the operator $\Re(\cdot)$ takes the real part of a complex number. This equation can be simplified into

$$\mathcal{S} = \pi \mathbf{H}_0^* \bar{\bar{\mu}}^i \mathbf{H}_0 \tag{3}$$

(see Appendix A for the detailed proof).

Applying successively the magnetic field in different directions, and setting $\mathcal{U} = \mathcal{S}$, the components of tensor $\bar{\bar{\mu}}^i$ can be obtained. Thus, heterogeneous anisotropic materials can be homogenized as a virtual homogeneous material. This material has a complex permeability tensor containing effective magnetic behavior and lossy features of SMC. In Section III, the tensor $\bar{\bar{\mu}}^i$ is built considering two simplified configurations for SMC.

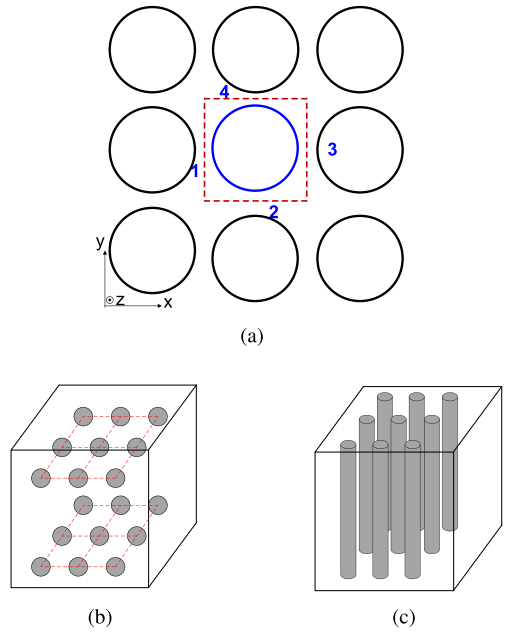

Fig. 1. (a) 2-D sketch of cubic lattice of spherical inclusions or square lattice of fiber inclusions. The domain confined by dashed lines 1–4 forms an elementary cell of periodic pattern. (b) 3-D view of cubic lattice of spherical inclusions (case 1). (c) 3-D view of square lattice of fiber inclusions (case 2).

III. Complex Permeability for SMC

SMC consists of inclusions surrounded by an insulating film. In this paper, attention is focused on two simple microstructures: cubic lattice of spherical inclusions and square lattice of fiber inclusions, as shown in Fig. 1. The fiber inclusion problem can be reduced to 2-D. Only circular cross section of fiber is considered.

Besides, in the following discussion, isotropic constituents are considered. The loading consists in a harmonic magnetic field at low-frequency range. Thus, the skin effect and the induced magnetic field are negligible. There are two steps to determine the complex permeability tensor. First, in the case of a single inclusion embedded in an infinite medium, the magnetic field in the inclusion is uniform. EC loss density is deduced as a function of this uniform field. Second, we introduce an imaginary part in the effective complex permeability tensor, related to the loss density.

For dilute SMC (low concentration of inclusions), each inclusion can be treated as in the single inclusion case. But as the volume fraction of inclusions increases, the internal field inside each inclusion is distorted by the neighboring inclusions. Under such conditions, the uniform field of the single inclusion case is replaced by the average field in the inclusion. EC loss density and imaginary part of complex permeability tensor are thus estimated.

A. Simple Case: Uniform Field in the Inclusion

If a magnetic inclusion of ellipsoidal or cylindrical shape is placed in an initially uniform magnetic field—and neglecting the induced field—the magnetic field $\mathbf{H}$ inside the inclusion is also uniform [33]: $\mathbf{H} = \mathbf{H}_i e^{j\omega t}$. Considering a nonconductive surrounding medium and an isotropic permeability μ and conductivity σ for the inclusion, the induced electric field $\mathbf{E}$ in the inclusion can be deduced using the following balance equations:

$$\begin{cases} \nabla \times \mathbf{E} = -j\omega\mu\mathbf{H} \\ \nabla \cdot (\sigma \mathbf{E}) = 0. \end{cases} \tag{4}$$

By substituting the induced field $\mathbf{E}$ into (1), the EC loss density can be further obtained

$$\mathcal{U} = \pi^2 R^2 f \sigma \mu^2 \mathbf{H}_i^* \bar{\bar{K}} \mathbf{H}_i \tag{5}$$

where R is the radius of the sphere or cylinder, and $\bar{\bar{K}}$ is a shape factor tensor: $\bar{\bar{K}} = (1/5)\bar{\bar{I}}$ for spherical inclusion with $\bar{\bar{I}}$ the matrix identity and $\bar{\bar{K}} = \Lambda((1/2), (1/2), (1/4))$ for cylindrical inclusion with $\Lambda(\cdot)$ representing a diagonal matrix (see Appendix B for the detailed proof).

Substituting (5) into (3) by $\mathcal{U} = \mathcal{S}$ leads to the following definition for the imaginary part of the inclusion permeability tensor:

$$\bar{\bar{\mu}}^i_{\text{inc}} = \pi R^2 f \sigma \mu^2 \bar{\bar{K}}. \tag{6}$$

Consider now the SMC material as a representative elementary cell containing an inclusion and its surrounding matrix. This cell has spatial periodicity. The properties of the inclusion are denoted with the subscript 2 and the properties of the matrix with the subscript 1. Although EC occurs only in the inclusion, the macroscopic EC (flowing in the matrix) being negligible, the idea of effective tensor is developed from the perspective of the whole representative cell.

For dilute SMC where the volume fraction v_2 of inclusions is sufficiently small, the magnetic field inside the inclusion can still be viewed as uniform. For biphasic composites, with effective magnetic permeability tensor $\bar{\bar{\mu}}^r$, the average field $\langle \mathbf{H} \rangle_2$ in the inclusion is given by [34]

$$\langle \mathbf{H} \rangle_2 = \frac{1}{v_2(\mu_2 - \mu_1)} (\bar{\bar{\mu}}^r - \mu_1 \bar{\bar{I}}) \langle \mathbf{H} \rangle \tag{7}$$

where $\langle \mathbf{H} \rangle$ is the average field over the whole cell. The effective magnetic permeability tensor $\bar{\bar{\mu}}^r$ can be retrieved using MG estimate [35]

$$\bar{\bar{\mu}}^r = \mu_1 \bar{\bar{I}} + v_2 \mu_1 (\mu_2 - \mu_1)[\mu_1 \bar{\bar{I}} + (1 - v_2)(\mu_2 - \mu_1)\bar{\bar{N}}]^{-1} \tag{8}$$

with the depolarization tensor $\bar{\bar{N}} = (1/3)\bar{\bar{I}}$ for spherical inclusions and $\bar{\bar{N}} = \Lambda((1/2), (1/2), 0)$ for cylindrical inclusions.

The EC loss density $\mathcal{U}_2$ in the inclusion can be written as a function of the—uniform—magnetic field in the inclusion ($\mathbf{H}_2 = \langle \mathbf{H} \rangle_2$)

$$\mathcal{U}_2 = \pi^2 R^2 f \sigma_2 \mu_2^2 \mathbf{H}_2^* \bar{\bar{K}} \mathbf{H}_2. \tag{9}$$

From the perspective of the whole composite material, the EC loss density $\mathcal{U}$ is then

$$\mathcal{U} = v_2 \mathcal{U}_2. \tag{10}$$

Combining (3) and (7)–(10) with $\mathcal{U} = \mathcal{S}$ gives the following expression for the imaginary part $\bar{\bar{\mu}}^i$ of the complex permeability tensor of the composite material:

$$\bar{\bar{\mu}}^i = v_2 \pi R^2 f \sigma_2 \mu_1^2 \mu_2^2 \bar{\bar{K}} [\mu_1 \bar{\bar{I}} + (1 - v_2)(\mu_2 - \mu_1)\bar{\bar{N}}]^{-2}. \tag{11}$$

B. Nonuniform Field in the Inclusion

For SMC with relatively high volume fraction v_2 of inclusions, the field in the inclusion cannot be considered uniform anymore. Equation (9) cannot be readily deduced as in the single inclusion case. Nevertheless, the assumption that (9) is still applicable is made, replacing $\mathbf{H}_2$ with the average field $\langle \mathbf{H} \rangle_2$ within the inclusions. Therefore, the EC loss density estimate for the whole composite becomes

$$\mathcal{U} = v_2 \pi^2 R^2 f \sigma_2 \mu_2^2 \langle \mathbf{H} \rangle_2^* \bar{\bar{K}} \langle \mathbf{H} \rangle_2. \tag{12}$$

Equation (7) can still be applied to calculate $\langle \mathbf{H} \rangle_2$. However, as the volume fraction v_2 increases, MG estimate brings unacceptable inaccuracy for the definition of the effective magnetic permeability (real part of the effective complex permeability tensor). This definition must then be revisited. In the special case of cylindrical inclusions with an applied magnetic field along the cylinder length, the magnetic field in the study domain is uniform, as long as the frequency is sufficiently low (no skin effect). In such case, Wiener estimate [36] provides an exact formula to compute the corresponding component of the effective magnetic permeability tensor. In other cases, $\bar{\bar{\mu}}^r$ has to be calculated either by FEM computation or by series expansions [8], [10]. The latter provides a high precision estimate if sufficiently high-order terms are computed (see Appendix C for equations).

For high volume fraction configurations, considering no overlapping between inclusions—consistently with SMC microstructure—macroscopic EC can still be neglected. Therefore, (10) is still applicable. Given $\bar{\bar{\mu}}^r$, combining (3), (7), and (12) with $\mathcal{U} = \mathcal{S}$ leads to

$$\bar{\bar{\mu}}^i = \frac{\pi R^2 f \sigma_2 \mu_2^2}{v_2 (\mu_2 - \mu_1)^2} \bar{\bar{K}} (\bar{\bar{\mu}}^r - \mu_1 \bar{\bar{I}})^2. \tag{13}$$

Equation (11) is only a particular case of (13), where the effective magnetic permeability (real part) is taken as the MG estimate. Tensor $\bar{\bar{\mu}}^i$ is proportional to the frequency f, to the inclusion conductivity σ_2 and also depends on the magnetic permeabilities μ_1 and μ_2 of the constituents, on the volume fraction v_2, size R, and shape factor tensor $\bar{\bar{K}}$ of the inclusions.

Finally, the complex permeability tensor $\tilde{\mu}$ for an SMC material is defined as

$$\tilde{\mu} = \bar{\bar{\mu}}^r - j \frac{\pi R^2 f \sigma_2 \mu_2^2}{v_2 (\mu_2 - \mu_1)^2} \bar{\bar{K}} (\bar{\bar{\mu}}^r - \mu_1 \bar{\bar{I}})^2. \tag{14}$$

The real part represents the magnetic behavior of the composite, and the imaginary part offers an immediate approach to calculate EC loss density, by (3). It must be noticed that an accurate estimate of the effective magnetic permeability tensor $\bar{\bar{\mu}}^r$ is required to define the effective complex permeability tensor $\tilde{\mu}$. Two critical points have to be studied in order to assess the validity of the approach: the first one is the applicability of (12) for high volume fraction materials, and the second one is the accuracy of the prediction of EC losses obtained from the complex permeability tensor $\tilde{\mu}$. This assessment will be performed in Section IV using FEM computations.

TABLE I
MATERIAL PARAMETERS USED IN THE CALCULATIONS FOR SMC

	Conductivity (S/m)	Relative Permeability	Relative Permittivity
Iron	1.12×10^7	4000	1
Epoxy	1.7×10^{-13}	1	9

IV. VALIDATION USING FEM COMPUTATIONS

The problem of 2-D SMC with a magnetic field applied in the normal direction has been discussed thoroughly [37], [38]. At low frequency, the magnetic field is uniform in the domain, so that (12) is an exact formula for EC losses in the inclusion. In this simple case, the effective magnetic permeability (real part) is obtained from the Wiener estimate, which also provides in that case an exact value. Therefore, the required validations concern the spherical inclusion case (later referred to as case 1), and the case of cylindrical inclusions with in-plane loading (later referred to as case 2). These two cases are associated with more complex field distributions, and require more advanced homogenization techniques.

To carry out this validation, FEM simulations have been performed on a unit cell of SMC, as described in Fig. 1(a), for different volume fractions v_2 at different frequencies. The cell size L_1 (lattice length) is fixed to 50 μm. The average flux density over a cell is imposed at $B_0 = 1$ T. FEM calculations are conducted with the commercial software COMSOL Multiphysics. The software runs on a workstation equipped with 4-core Intel Xeon CPU at 3.7 GHz and 128 GB memory. Vector magnetic potential $\mathbf{A}$ formulation is employed. For boundary conditions, the magnetic flux is imposed on two surfaces, and perfect magnetic conductor determined by $\mathbf{n} \times \mathbf{H} = 0$ and $\mathbf{n} \cdot \mathbf{J} = 0$ is imposed otherwise.

For case 1 computations, for symmetry reasons, only half of the unit cell is modeled. The magnetic field is directed along the z-axis. A 3-D mesh made of hexahedral elements has been used. The mesh is constituted of approximately one million elements. The computation time is about 300 s. For case 2 computations, the magnetic field is applied along the y-axis. A 2-D mesh made of triangular elements has been used. The mesh is constituted of approximately 3×10^4 elements. The computation time is about 2 s. The material properties used for the constituents are given in Table I.

The total EC loss density $\mathcal{U}_n$ and the average value $\langle \mathbf{H} \rangle_{2n}$ of the magnetic field in the inclusion are post-processed (the subscript n refers to a numerical FEM result). $\langle \mathbf{H} \rangle_{2n}$ is introduced into (12) to get the EC loss density approximation $\mathcal{U}_a$. The comparison between $\mathcal{U}_a$ and $\mathcal{U}_n$ indicates the validity of the average field assumption in (12).

In the following, the effective magnetic permeability (real part) is calculated according to the series expansion given in Appendix C. The EC loss density estimated by the homogenization model is noted $\mathcal{U}_h$. It is obtained analytically from (3) after the complex permeability tensor model has been used. The comparison between $\mathcal{U}_n$ and $\mathcal{U}_h$ indicates the validity of the proposed model. This comparison has been performed for different concentrations of inclusions and different values of magnetic permeability for the inclusions.

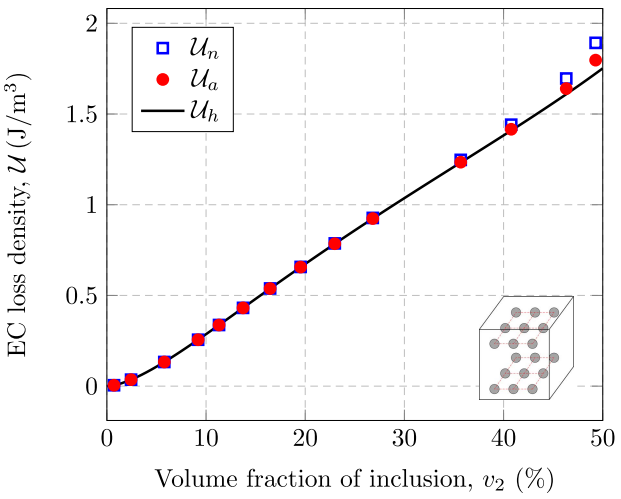

(a)

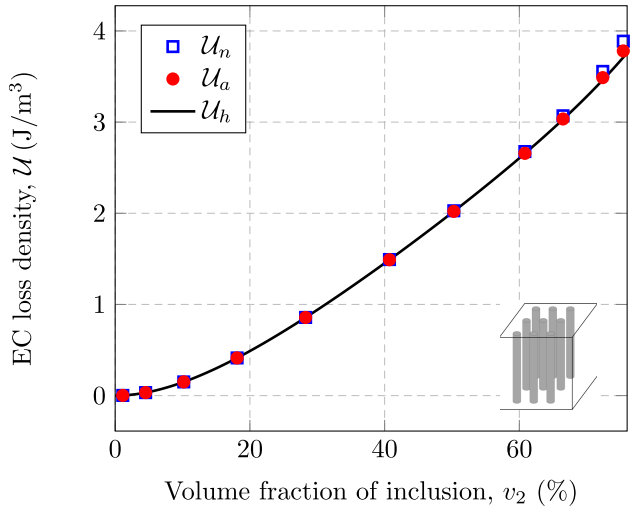

(b)

Fig. 2. EC loss density as a function of inclusion volume fraction evaluated by full FEM computation (squares), by approximation (12) using the average magnetic field obtained by FEM (circles), and by the proposed analytical formulation (line). (a) Cubic lattice of spheres: magnetic field loading along the z-direction (case 1). (b) Square lattice of fibers: in-plane loading field along the y-direction (case 2). For all calculations: frequency $f = 100$ Hz, lattice size $L_1 = 50$ μm, $\mu_2 = 4000\mu_0$, $\mu_1 = \mu_0$, $\sigma_2 = 1.12 \times 10^7$ S/m, and average flux density $B_0 = 1$.

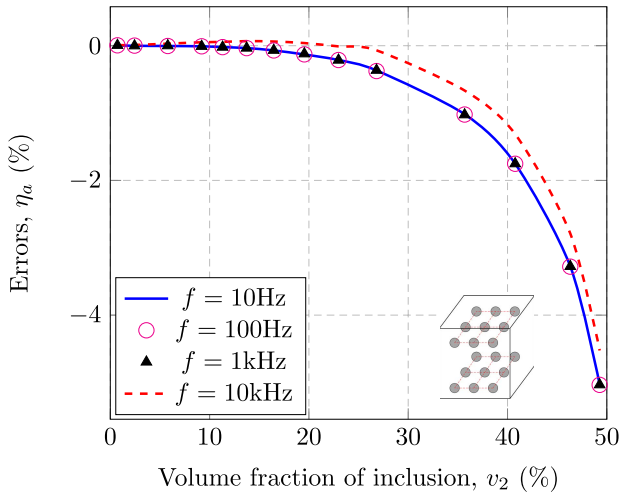

(a)

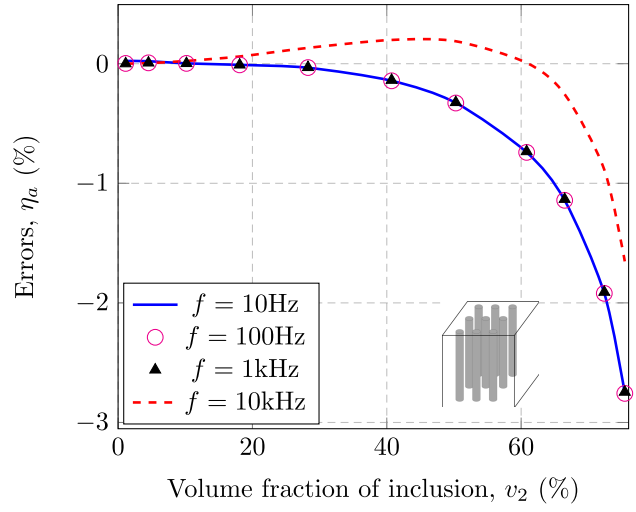

(b)

Fig. 3. Errors on EC losses attributed to the average field assumption in (12) as a function of volume fraction v_2 for different frequencies. (a) Cubic lattice of spheres: magnetic field loading along the z-direction (case 1). (b) Square lattice of fibers: in-plane loading field along the y-direction (case 2). For all calculations: lattice size $L_1 = 50$ μm, $\mu_2 = 4000\mu_0$, $\mu_1 = \mu_0$, $\sigma_2 = 1.12 \times 10^7$ S/m, and average flux density $B_0 = 1$ T.

Fig. 2 shows the EC loss density as a function of the volume fraction v_2 of the inclusions, in both case 1 (spherical inclusions) and case 2 (fiber inclusions and in-plane magnetic field).

As expected—since the flux is imposed—EC losses increase when the volume fraction of inclusions becomes higher. At low volume fraction, the average field assumption and the analytical formulation are consistent with the FEM results. As the volume fraction increases, discrepancies arise. These discrepancies can be attributed to two main causes. The first is the assumption used in relation (12) that the average magnetic field within the inclusions can be used to estimate the EC losses. The second is the definition of the complex permeability tensor $\tilde{\mu}$ based on the proposed homogenization model. These causes can be studied separately by considering successively the estimates $\mathcal{U}_a$ and $\mathcal{U}_h$ for EC losses.

A. Average Field Assumption

The error related to the average field assumption is defined as

$$\eta_a = \frac{\mathcal{U}_a - \mathcal{U}_n}{\mathcal{U}_n} \times 100\%. \tag{15}$$

Fig. 3 shows the evolution of η_a as a function of the volume fraction v_2 for the two studied cases at frequencies from 10 Hz to 10 kHz.

The error level increases with the volume fraction v_2. At low volume fraction, the errors tend toward zero, which is consistent with the dilute approximation with quasi-uniform field inside the inclusions. On the other hand, as the volume fraction increases, the field distortion becomes more and more significant, and the error η_a increases. Fig. 3 also shows that for the studied cases, (12) underestimates the losses. At low

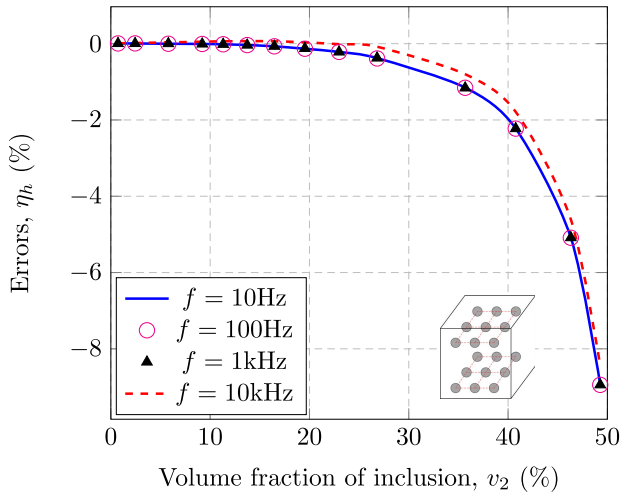

(a)

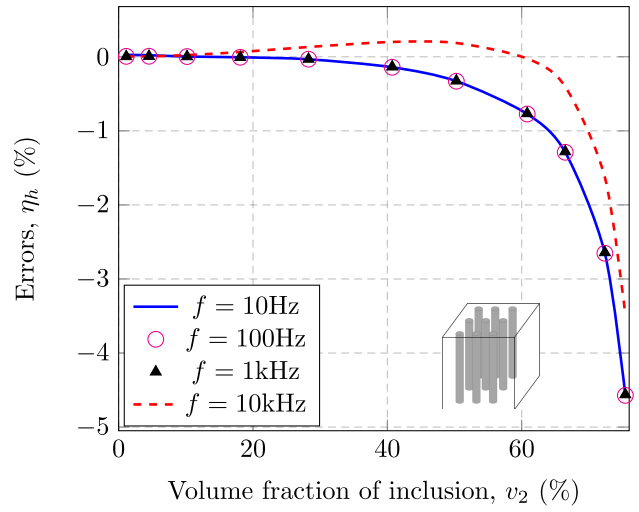

(b)

Fig. 4. Errors on EC losses of the proposed homogenization model as a function of volume fraction v_2 for different frequencies. (a) Cubic lattice of spheres: magnetic field loading along the z-direction (case 1). (b) Square lattice of fibers: in-plane loading field along the y-direction (case 2). For all calculations: lattice size $L_1 = 50$ μm, $\mu_2 = 4000\mu_0$, $\mu_1 = \mu_0$, $\sigma_2 = 1.12 \times 10^7$ S/m, and average flux density $B_0 = 1$ T.

frequency (lower than 1 kHz), the error does not depend on frequency. For higher frequencies, the induced magnetic field cannot be neglected anymore. The induced magnetic field reduces the level of the whole magnetic field leading to a reduction of the losses in the numerical computation. This reduces the difference between $\mathcal{U}_a$ and $\mathcal{U}_n$, because the average field approximation tends to underestimate the loss level. This effect explains the reduction of the error observed at high frequency.

Overall, the average field approximation brings errors lower than 5% on the EC losses estimate, which validates the applicability of (12).

B. Effective Complex Permeability Tensor

Another source of error in the full homogenization approach is the definition of the complex permeability tensor that adds

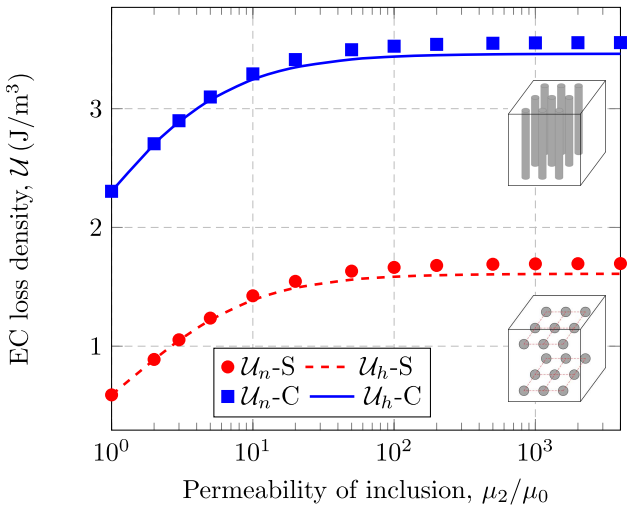

Fig. 5. EC loss density $\mathcal{U}_h$ evaluated with the proposed approach (lines) for cases 1 and 2 and corresponding FEM results $\mathcal{U}_n$ (dots) as a function of the permeability contrast between matrix and inclusions. For all calculations: $f = 100$ Hz, lattice size $L_1 = 50$ μm, $R = 24$ μm, $\mu_1 = \mu_0$, $\sigma_2 = 1.12 \times 10^7$ S/m, and average flux density $B_0 = 1$ T.

up to the error discussed in Section IV-A. The total error of the model is defined as

$$\eta_h = \frac{\mathcal{U}_h - \mathcal{U}_n}{\mathcal{U}_n} \times 100\%. \tag{16}$$

Fig. 4 shows the evolution of η_h as a function of the volume fraction v_2 for the two studied cases at frequencies from 10 Hz to 10 kHz.

The trend on the error η_h is very similar to that of η_a. The definition of the effective complex permeability tensor just increases the general level of error, approximately by a factor 2. This increase in the error level could be reduced to almost zero by increasing the order of the series expansion used to calculate the effective permeability (see Appendix C). But this comes to a higher computation cost.

The level of error is also a function of the permeability contrast between matrix and inclusions. The matrix magnetic permeability is kept as μ_0. The error being frequency-independent at low frequency (see Figs. 3 and 4), the frequency is fixed at $f = 100$ Hz. The radius R for the inclusions is also fixed at $R = 24$ μm corresponding to a volume fraction of 46.3% for spherical inclusions (case 1) and 72.4% for cylindrical inclusions (case 2). The EC loss density as a function of the permeability contrast between matrix and inclusions is given in Fig. 5. The corresponding error η_h is given in Fig. 6. The EC loss density increases with the permeability of the inclusions. It reaches a saturation value when the permeability contrast is greater than 100.

These results show that, when the permeability contrast is high, greater than a few hundreds, the error remains at a very stable level, lower than 6% and 3% for case 1 and case 2, respectively. As the contrast decreases, the error decreases, which is expected because the distortion of the magnetic field inside the inclusions is higher when the contrast is higher. In other words, the average field assumption

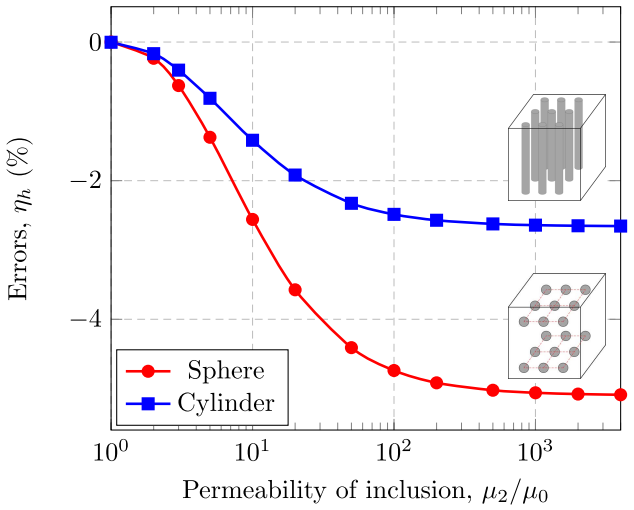

Fig. 6. Errors on EC losses of the proposed homogenization model as a function of the permeability contrast between matrix and inclusions for cases 1 and 2. For all calculations: $f = 100$ Hz, lattice size $L_1 = 50$ μm, $R = 24$ μm, $\mu_1 = \mu_0$, $\sigma_2 = 1.12 \times 10^7$ S/m, and average flux density $B_0 = 1$ T.

is getting more and more appropriate when the contrast is low.

V. Conclusion

In this paper, a homogenization strategy for SMCs is proposed. The purpose is to define an effective complex permeability tensor representative for the behavior of the material. The real part of this tensor reflects the magnetic behavior of the composite, while the imaginary part reflects the EC losses. This imaginary part is proportional to the loading frequency and depends on the magnetic permeability tensor of each constituent of the composite, on the inclusion concentration, on the size and conductivity of the inclusions, where ECs are generated, and on the spatial arrangement of inclusions, which eventually determines the magnetic field distribution within the structure.

Based on the study of a single inclusion in an infinite medium, the case of dilute heterogeneous materials is deduced, and the general case of composites is extrapolated from this approach. As a result, EC loss density in SMCs is described using a homogenized complex permeability tensor. The approach is compared with the FE results, and the observed errors are of the order of 5%. It is worth noting that the approach requires accurate estimates of the effective static magnetic permeability tensor of the composite material. It is found that the approach tends to underestimate the EC loss density compared with the FE results, and that the errors are frequency-independent for frequencies below 1 kHz.

The microstructures considered in this paper are not fully representative for real SMC, and limit the filling factors that can be achieved. Higher filling factors, hence, more complex shapes for the inclusions must be considered. The same approach remains applicable, the keypoint lying in the determination of the effective magnetic permeability and of the average magnetic field in the inclusion. This is part of a work in progress, and further comparisons with FE computations will be carried out.

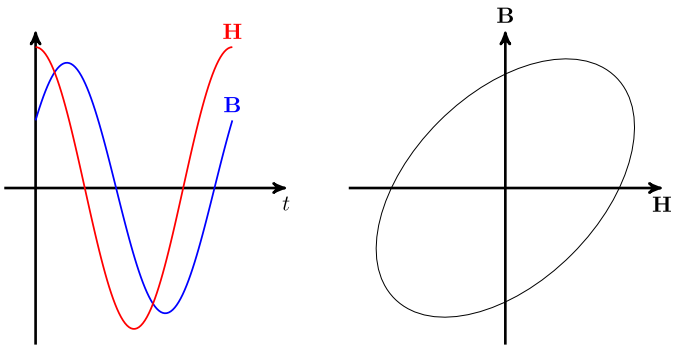

Fig. 7. Phase shift between **B** and **H**, forming an ellipse in a period time. The area of this ellipse is the energy density during one time period.

Appendix A
Energy Density

This Appendix is the proof of (3), recalled hereafter, giving the energy loss density for a homogeneous and linear magnetic material under sinusoidal excitation

$$\mathcal{S} = \pi \mathbf{H}_0^* \bar{\bar{\mu}}^i \mathbf{H}_0. \tag{17}$$

Consider a homogeneous and linear material of permeability tensor $\bar{\bar{\mu}}^r$ excited by a harmonic magnetic field $\mathbf{H}(t) = \mathbf{H}_0 e^{j\omega t}$ ($\mathbf{H}_0$ is the magnetic field magnitude and ω is the angle frequency). Locally, the magnetic behavior of the material is given by $\mathbf{B}(t) = \bar{\bar{\mu}}^r \mathbf{H}(t)$. There is no hysteresis loss in magnetic linear materials. For quasi-static magnetic fields, the phase shift between $\mathbf{B}(t)$ and $\mathbf{H}(t)$ is negligible. If we introduce an imaginary part in the permeability tensor, $\mathbf{B}(t)$ and $\mathbf{H}(t)$ now exhibit a phase shift, as shown in Fig. 7. In a period of time, $\mathbf{B}(t)$ and $\mathbf{H}(t)$ form an ellipse. The area of this ellipse is the energy density during one period. We can make use of this energy density to represent the EC loss density. Consider a complex magnetic permeability tensor $\tilde{\mu} = \bar{\bar{\mu}}^r - j\bar{\bar{\mu}}^i$, where $\bar{\bar{\mu}}^r$ is the usual material magnetic permeability tensor. The area of the **B**-**H** ellipse is directly connected to the imaginary part of the complex permeability tensor, so that $\bar{\bar{\mu}}^i$ can be assigned to the description of the EC loss density.

To obtain the area of the ellipse, a classical integration is performed over a period of time T

$$\begin{aligned}\mathcal{S} &= \frac{1}{2}\Re\left(\int_0^T \mathbf{H}^*(t)\frac{d\mathbf{B}(t)}{dt}\,dt\right)\\ &= \frac{1}{2}\Re\left(\int_0^T \mathbf{H}_0^* e^{-j\omega t} j\omega\tilde{\mu}\mathbf{H}_0 e^{j\omega t}\,dt\right)\\ &= \frac{1}{2}\Re\left(2\pi\mathbf{H}_0^*(j\bar{\bar{\mu}}^r + \bar{\bar{\mu}}^i)\mathbf{H}_0\right)\\ &= \pi\mathbf{H}_0^*\bar{\bar{\mu}}^i\mathbf{H}_0.\end{aligned} \tag{18}$$

Equation (3) is finally retrieved. This result can also be found in [32].

Appendix B
Shape Factor Tensors

This Appendix gives the proof for the expressions of the energy loss density in single inclusions embedded in an

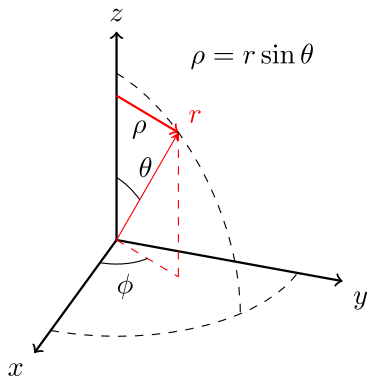

Fig. 8. Cylindrical and spherical coordinates.

infinite medium. The main aspect is the definition of the shape factor tensor $\bar{\bar{K}}$ as a function of the inclusion shape. Three cases are treated separately: spherical inclusion, cylindrical inclusion with in-plane loading, and cylindrical inclusion with normal loading. The shape factor tensors for spherical and cylindrical inclusions are deduced from these calculations.

A. Spherical Inclusion

We consider cylindrical coordinates (ρ, ϕ, z). The magnetic field is applied along the z-axis. Since the magnetic field ($\mathbf{H} = [0, 0, H_0]^t$) is uniform within the sphere (radius R), the induced electric field rotates around the z-axis. Considering a cross section Ω normal to the z-axis, the equation $\nabla \times \mathbf{E} = -j\omega\mu\mathbf{H}$ is solved in the domain Ω. We have

$$\frac{1}{\rho}\frac{\partial(\rho E_\phi)}{\partial\rho} = -j\omega\mu H_0. \tag{19}$$

Then, considering $E_\phi = 0$ at the center of Ω, we obtain

$$E_\phi(\rho, \phi, z) = -\frac{1}{2}j\omega\mu H_0\rho. \tag{20}$$

This field $\mathbf{E}(\rho, \phi, z)$ is then transformed from cylindrical coordinates to spherical coordinates (r, ϕ, θ), as indicated in Fig. 8. The electric field is then expressed as

$$\mathbf{E}(r, \phi, \theta) = -\frac{1}{2}j\omega\mu H_0 r \sin\theta\vec{u}_\phi \tag{21}$$

where $\vec{u}_\phi$ is a unit vector.

Therefore, the loss density can be expressed as

$$\mathcal{U} = \frac{\langle\mathbf{E}^*\bar{\bar{\sigma}}\mathbf{E}\rangle}{2f} = \frac{\pi^2}{5}R^2 f\sigma\mu^2 H_0^2. \tag{22}$$

This result can also be found in [39]. Using the symmetries of the problem, the shape factor tensor for the sphere is then defined as

$$\bar{\bar{K}} = \frac{1}{5}\bar{\bar{I}}. \tag{23}$$

B. Cylindrical Inclusion (Circle) With In-Plane Loading

We consider a Cartesian coordinate system xOy, and a circle with center O and radius R. The magnetic field is applied along the y-axis. Since the magnetic field ($\mathbf{H} = [0, H_0, 0]^t$) is uniform within the circle, and considering the z-invariance of the problem, the induced electric field $\mathbf{E}$ is directed along the z-axis. The equation $\nabla \times \mathbf{E} = -j\omega\mu\mathbf{H}$ is solved in the circle to obtain the electric field

$$\mathbf{E}(x, y, z) = -j\omega\mu H_0 x\vec{u}_z. \tag{24}$$

This electric field $\mathbf{E}(x, y, z)$ is then transformed from Cartesian coordinates to cylindrical coordinates (ρ, ϕ, z)

$$\mathbf{E}(\rho, \phi, z) = -j\omega\mu H_0\rho\cos\phi\vec{u}_z. \tag{25}$$

Hence, the loss density is

$$\mathcal{U} = \frac{\langle\mathbf{E}^*\bar{\bar{\sigma}}\mathbf{E}\rangle}{2f} = \frac{\pi^2}{2}R^2 f\sigma\mu^2 H_0^2. \tag{26}$$

C. Cylindrical Inclusion (Circle) With Normal Loading

The previous configuration is kept, but the loading field is now normal to the plane (along the z-axis). The magnetic field $\mathbf{H} = [0, 0, H_0]^t$ inside the circle is still uniform. The equation $\nabla\times\mathbf{E} = -j\omega\mu\mathbf{H}$ is solved in the circle to obtain the following expression of the electric field:

$$\mathbf{E}(\rho, \phi, z) = -\frac{1}{2}j\omega\mu H_0\rho\vec{u}_\phi. \tag{27}$$

Hence, the loss density is

$$\mathcal{U} = \frac{\langle\mathbf{E}^*\bar{\bar{\sigma}}\mathbf{E}\rangle}{2f} = \frac{\pi^2}{4}R^2 f\sigma\mu^2 H_0^2. \tag{28}$$

This result can also be found in [37]. Synthesizing (26) and (28), the shape factor tensor for cylindrical inclusion can be written

$$\bar{\bar{K}} = \Lambda\left(\frac{1}{2}, \frac{1}{2}, \frac{1}{4}\right) = \begin{bmatrix} \frac{1}{2} & 0 & 0 \\ 0 & \frac{1}{2} & 0 \\ 0 & 0 & \frac{1}{4} \end{bmatrix}. \tag{29}$$

Appendix C
Determination of the Effective Magnetic Permeability (Real Part)

For cubic lattice of spherical inclusions or square lattice of circular inclusions, the effective magnetic permeability can be accurately determined using series expansions [8], [10]. The accuracy depends on the order of the terms of the series used for the practical calculation. In the case of spherical or circular inclusions, because of spatial symmetries, the effective magnetic permeability is isotropic. It is denoted by μ^r. The approximation used in this paper leads to the following expressions for μ^r:

$$\begin{cases} \mu^r = \left(1 + \dfrac{3v_2}{\gamma(v_2)}\right)\mu_1 & \text{(sphere)} \\ \mu^r = \dfrac{1 + \lambda(v_2)v_2}{1 - \lambda(v_2)v_2}\mu_1 & \text{(circle)} \end{cases} \tag{30}$$

where

$$\gamma(v_2) = -1/R_1 - v_2 + 1.3045R_3 v_2^{10/3} + 0.0723R_5 v_2^{14/3} - 0.5289R_3^2 v_2^{17/3} + 0.1526R_7 v_2^6 + O(v_2^7) \tag{31}$$

with

$$R_n = \frac{n(\mu_1 - \mu_2)}{(n+1)\mu_1 + n\mu_2} \tag{32}$$

and

$$\begin{aligned}\lambda(v_2) = \alpha &+ 0.305827\alpha^3 v_2^4 \\ &+ \alpha^3(0.0935304\alpha^2 + 0.0133615)v_2^8 \\ &+ \alpha^3(0.0286042\alpha^4 + 0.437236\alpha^2 \\ &\qquad + 0.000184643)v_2^{12} \\ &+ O(v_2^{16})\end{aligned} \tag{33}$$

with

$$\alpha = \frac{\mu_2 - \mu_1}{\mu_2 + \mu_1}. \tag{34}$$

The theoretical foundations for these expressions can be found in [8] and [10].

ACKNOWLEDGMENT

X. Ren is a fellowship beneficiary with the cooperation program between the China Scholarship Council and Université Paris-Sud.

REFERENCES

[1] G. Cvetkovski and L. Petkovska, "Performance improvement of PM synchronous motor by using soft magnetic composite material," *IEEE Trans. Magn.*, vol. 44, no. 11, pp. 3812–3815, Nov. 2008.

[2] A. Chebak, P. Viarouge, and J. Cros, "Analytical computation of the full load magnetic losses in the soft magnetic composite stator of high-speed slotless permanent magnet machines," *IEEE Trans. Magn.*, vol. 45, no. 3, pp. 952–955, Mar. 2009.

[3] F. Bernot, A. Bernot, and J.-C. Vannier, "A synchronous wound excitation transverse flux machine with solid rotor," in *Innovative Design, Analysis and Development Practices in Aerospace and Automotive Engineering*. New Delhi, India: Springer, 2014, pp. 25–39.

[4] T. Sato, S. Aya, H. Igarashi, M. Suzuki, Y. Iwasaki, and K. Kawano, "Loss computation of soft magnetic composite inductors based on interpolated scalar magnetic property," *IEEE Trans. Magn.*, vol. 51, no. 3, Mar. 2015, Art. no. 8001704.

[5] H. Shokrollahi and K. Janghorban, "Soft magnetic composite materials (SMCs)," *J. Mater. Process. Technol.*, vol. 189, nos. 1–3, pp. 1–12, 2007.

[6] L. Rayleigh, "On the influence of obstacles arranged in rectangular order upon the properties of a medium," *Philos. Mag.*, vol. 34, no. 211, pp. 481–502, 1892.

[7] R. C. McPhedran and D. R. McKenzie, "The conductivity of lattices of spheres. I. The simple cubic lattice," *Proc. Roy. Soc. London. Ser. A, Math. Phys. Sci.*, vol. 359, no. 1696, pp. 45–63, 1978.

[8] J. Lam, "Magnetic permeability of a simple cubic lattice of conducting magnetic spheres," *J. Appl. Phys.*, vol. 60, no. 12, pp. 4230–4235, 1986.

[9] B. Y. Balagurov and V. A. Kashin, "The conductivity of a 2D system with a doubly periodic arrangement of circular inclusions," *Tech. Phys.*, vol. 46, no. 1, pp. 101–106, 2001.

[10] Y. A. Godin, "Effective complex permittivity tensor of a periodic array of cylinders," *J. Math. Phys.*, vol. 54, no. 5, p. 053505, 2013.

[11] A. Bossavit, "On the homogenization of Maxwell equations," *COMPEL—Int. J. Comput. Math. Electr. Electron. Eng.*, vol. 14, no. 4, pp. 23–26, 1995.

[12] M. El Feddi, Z. Ren, A. Razek, and A. Bossavit, "Homogenization technique for Maxwell equations in periodic structures," *IEEE Trans. Magn.*, vol. 33, no. 2, pp. 1382–1385, Mar. 1997.

[13] G. Meunier, V. Charmoille, C. Guérin, P. Labie, and Y. Maréchal, "Homogenization for periodical electromagnetic structure: Which formulation?" *IEEE Trans. Magn.*, vol. 46, no. 8, pp. 3409–3412, Aug. 2010.

[14] I. Niyonzima, R. Sabariego, P. Dular, and C. Geuzaine, "Finite element computational homogenization of nonlinear multiscale materials in magnetostatics," *IEEE Trans. Magn.*, vol. 48, no. 2, pp. 587–590, Feb. 2012.

[15] O. Bottauscio and A. Manzin, "Comparison of multiscale models for eddy current computation in granular magnetic materials," *J. Comput. Phys.*, vol. 253, pp. 1–17, Nov. 2013.

[16] G. W. Milton, *The Theory of Composites*. Cambridge, U.K.: Cambridge Univ. Press, 2002.

[17] G. Papanicolau, A. Bensoussan, and J.-L. Lions, *Asymptotic Analysis for Periodic Structures* (Studies in Mathematics and Its Applications). Amsterdam, The Netherlands: Elsevier, 1978.

[18] M. Chiampi and D. Chiarabaglio, "Investigation on the asymptotic expansion technique applied to electromagnetic problems," *IEEE Trans. Magn.*, vol. 28, no. 4, pp. 1917–1923, Jul. 1992.

[19] C. Conca and S. Natesan, "Numerical methods for elliptic partial differential equations with rapidly oscillating coefficients," *Comput. Methods Appl. Mech. Eng.*, vol. 192, pp. 47–76, Jan. 2003.

[20] P. Queffelec, D. Bariou, and P. Gelin, "A predictive model for the permeability tensor of magnetized heterogeneous materials," *IEEE Trans. Magn.*, vol. 41, no. 1, pp. 17–23, Jan. 2005.

[21] L. Daniel and R. Corcolle, "A note on the effective magnetic permeability of polycrystals," *IEEE Trans. Magn.*, vol. 43, no. 7, pp. 3153–3158, Jul. 2007.

[22] C. L. Holloway, M. S. Sarto, and M. Johansson, "Analyzing carbon-fiber composite materials with equivalent-layer models," *IEEE Trans. Electromagn. Compat.*, vol. 47, no. 4, pp. 833–844, Nov. 2005.

[23] F. Qin and C. Brosseau, "A review and analysis of microwave absorption in polymer composites filled with carbonaceous particles," *J. Appl. Phys.*, vol. 111, no. 6, p. 061301, 2012.

[24] V. Préault, R. Corcolle, L. Daniel, and L. Pichon, "Effective permittivity of shielding composite materials for microwave frequencies," *IEEE Trans. Electromagn. Compat.*, vol. 55, no. 6, pp. 1178–1186, Dec. 2013.

[25] J. C. M. Garnett, "Colours in metal glasses and in metallic films," *Philos. Trans. Roy. Soc. London*, vol. 203, pp. 385–420, Jan. 1904.

[26] C. Brosseau and A. Beroual, "Computational electromagnetics and the rational design of new dielectric heterostructures," *Prog. Mater. Sci.*, vol. 48, no. 5, pp. 373–456, 2003.

[27] C. Brosseau, "Modelling and simulation of dielectric heterostructures: A physical survey from an historical perspective," *J. Phys. D, Appl. Phys.*, vol. 39, no. 7, p. 1277, 2006.

[28] B. Sareni, L. Krähenbühl, A. Beroual, and C. Brosseau, "Complex effective permittivity of a lossy composite material," *J. Appl. Phys.*, vol. 80, no. 8, pp. 4560–4565, 1996.

[29] K. G. N. B. Abeywickrama, T. Daszczynski, Y. V. Serdyuk, and S. M. Gubanski, "Determination of complex permeability of silicon steel for use in high-frequency modeling of power transformers," *IEEE Trans. Magn.*, vol. 44, no. 4, pp. 438–444, Apr. 2008.

[30] H. Hamzehbahmani, P. Anderson, J. Hall, and D. Fox, "Eddy current loss estimation of edge burr-affected magnetic laminations based on equivalent electrical network—Part I: Fundamental concepts and FEM modeling," *IEEE Trans. Power Del.*, vol. 29, no. 2, pp. 642–650, Apr. 2014.

[31] O. Moreau, L. Popiel, and J. L. Pages, "Proximity losses computation with a 2D complex permeability modelling," *IEEE Trans. Magn.*, vol. 34, no. 5, pp. 3616–3619, Sep. 1998.

[32] X. Nan and C. R. Sullivan, "A two-dimensional equivalent complex permeability model for round-wire windings," in *Proc. IEEE 36th Power Electron. Specialists Conf.*, Recife, Brazil, Jun. 2005, pp. 613–618.

[33] J. A. Stratton, *Electromagnetic Theory*. Hoboken, NJ, USA: Wiley, 2007.

[34] R. Corcolle, L. Daniel, and F. Bouillault, "Intraphase fluctuations in heterogeneous magnetic materials," *J. Appl. Phys.*, vol. 105, no. 12, p. 123913, 2009.

[35] A. Sihvola, *Electromagnetic Mixing Formulas and Applications* (Electromagnetics and Radar Series), vol. 47. London, U.K.: IEE, 1999.

[36] O. Wiener, *Die Theorie des Mischkörpers für das Feld der Stationären Strömung. 1 Die Mittelwertsätze für Kraft, Polarisation und Energie* (Abhandlungen der Königlich-Sächsischen Gesellschaft der Wissenschaften), vol. 1. Leipzig, Germany: B. G. Teubner, 1912.

[37] O. de la Barriere, M. LoBue, and F. Mazaleyrat, "Semianalytical and analytical formulas for the classical loss in granular materials with rectangular and elliptical grain shapes," *IEEE Trans. Magn.*, vol. 50, no. 10, pp. 1–8, Oct. 2014.

[38] X. Ren, R. Corcolle, and L. Daniel, "A 2D finite element study on the role of material properties on eddy current losses in soft magnetic composites," *Eur. Phys. J. Appl. Phys.*, vol. 73, no. 2, p. 20902, 2016.

[39] R. M. Bozorth, *Ferromagnetism*. Hoboken, NJ, USA: Wiley, 2003.